Groennings, S., ANAL. CHEM. 28, 303 (1956).
(5) Heilbron, I. M., Kamm, E. D., Owens, W. M., *J. Chem. Soc.* 1926, 1631.
(6) Isler, O., Rüegg, R., Chopard-dit-Jean, L., Bernhard, K., *Helv. Chim. Acta* 39, 897 (1956).
(7) Karrer, P., Helfenstein, A., *Ibid.*, 14, 78 (1931).
(8) Sax, K. J., Stross, F. H., *J. Org. Chem.* 22, 1251 (1957).
(9) Schmitt, J., *Ann.* 547, 115 (1941).
(10) Trippett, S., *Chem. & Ind. (London)* 1956, 80.
(11) Tsujimoto, M., *Ind. Eng. Chem.* 8, 889 (1916).
(12) Tunnicliff, D. D., Stone, H., ANAL. CHEM. 27, 73 (1955).

RECEIVED for review January 15, 1957. Accepted July 8, 1957.

Reaction Kinetics in Differential Thermal Analysis

HOMER E. KISSINGER

National Bureau of Standards, Washington, D. C.

▶ *The effects of the kinetics of reactions of the type solid → solid + gas on the corresponding differential thermal analysis pattern are explored. Curves of reaction rate vs. temperature for constant heating rates constructed by analytical methods are used to demonstrate the effect of varying order of reaction. The information so obtained is used to analyze the differential thermal patterns of magnesite, calcite, brucite, kaolinite, and halloysite. The results of the differential thermal study agree with results obtained isothermally except in some specific cases.*

WHEN a reaction occurs in differential thermal analysis (DTA), the change in heat content and in the thermal properties of the sample is indicated by a deflection, or peak. If the reaction proceeds at a rate varying with temperature—i.e., possesses an activation energy—the position of the peak varies with the heating rate if other experimental conditions are maintained fixed. In a previous paper (*10*), it was demonstrated that this variation in peak temperature could be used to determine the energy of activation for first order reactions. The present paper extends the method to reactions of any order, and proposes a method for determining the order of reaction from the shape of the differential thermal analysis peak.

DIFFERENTIAL TEMPERATURE AND REACTION RATE

In previous work it was assumed that the temperature of maximum deflection in differential thermal analysis is also the temperature at which the reaction rate is a maximum. Because the proposed method for determining kinetic constants depends on the accuracy of this assumption, a more detailed discussion of its validity is given.

The temperature distribution in the differential thermal analysis specimen holders obeys the general heat flow equation (*11*).

$$\frac{\partial T}{\partial t} - \frac{k}{\rho c}\nabla^2 T = \frac{1}{\rho c}\frac{dq}{dt} \qquad (1)$$

where T is the temperature, t the time, k the thermal conductivity, ρ the density, c the specific heat, and dq/dt the rate of heat generation due to a chemical reaction per unit volume of sample. No heat effects occur in the reference sample, so the temperature distribution in the reference is given by:

$$\frac{\partial T}{\partial t} = \frac{k}{\rho c}\nabla^2 T \qquad (2)$$

If the sample is assumed to be a cylinder of radius a and of infinite length, with the temperature of the outside given by $T = T_o + \phi t$, where ϕ is a constant rate of temperature rise and T_o the initial temperature, the temperature at T_r at the center of the reference sample is, by integration of Equation 2 with proper limits,

$$T_r = T_o + \phi t - \frac{\phi \rho c a^2}{4k} \qquad (3)$$

In Equation 1, the rate of heat generation is a function of temperature in the active sample. The equation then is a nonlinear partial differential equation, and cannot be solved by known analytical methods. We assume that, if the same boundary condition holds—i.e., that the temperature of the outside of the holder rises at a linear rate—the solution expressing the temperature at the center of the sample will be of the form:

$$T_s = T_h + \phi t - f\left(\frac{dq}{dt}\right) \qquad (4)$$

where $f\left(\frac{dq}{dt}\right)$ is a function of the reaction rate which also includes any secondary effects of the reaction, such as changes in volume, density, or thermal properties.

The differential temperature is the difference in temperature of the centers of the two samples. The differential temperature, θ, is then given by

$$\theta = f\left(\frac{dq}{dt}\right)_{\text{sample}} - \left(\frac{\phi \rho c a^2}{4k}\right)_{\text{reference}} \qquad (5)$$

and

$$\frac{d\theta}{dt} = f'\left(\frac{dq}{dt}\right)\frac{d^2q}{dt^2} \qquad (6)$$

When θ is a maximum, $d\theta/dt$ is zero. From Equation 6 it is seen that when d^2q/dt^2, the derivative of the rate of heat absorption, is zero, $d\theta/dt$ is also zero. Since the rate of heat absorption is proportional to the rate of reaction, Equation 6 states that the peak differential deflection occurs when the reaction rate is a maximum. This is true only when the heating rate of the reference is constant, as otherwise Equation 6 would contain a derivative of ϕ.

A solution of the form of Equation 3 can be obtained for a sample of any shape. If the reference material is thermally inert, the heating rate will be the same throughout the sample after quasi-steady state conditions have been established. Equation 6 is thus valid for any sample shape.

TEMPERATURE OF MAXIMUM DEFLECTION

Most reactions of the type solid → solid + gas can be described by an equation

$$\frac{dx}{dt} = A(1 - x)^n e^{-\frac{E}{RT}} \qquad (7)$$

where dx/dt is the rate, x is the fraction reacted, n is the empirical order of reaction, and T is the Kelvin temperature.

Reactions of this type may take place by one of a number of elementary mechanisms, as well as combinations of these mechanisms. In most cases which have been studied, the exponent n in Equation 7 is unity or fractional, and remains constant through the greater part of the reaction. The results of studies of solid decomposition mechanisms are summarized by Garner (*4*). In the present paper it is assumed that n remains constant.

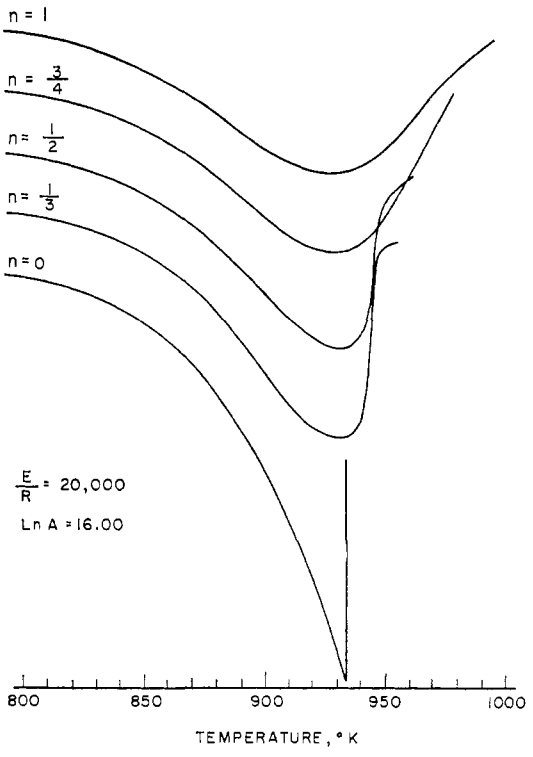

Figure 1. Effect of order of reaction on plots of reaction-rate vs. temperature for constant heating rate, frequency factor, and activation energy

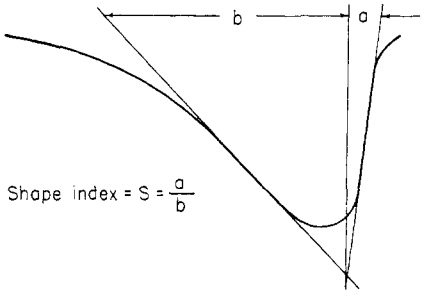

Figure 2. Method for measuring amount of asymmetry in an endothermic differential thermal analysis peak

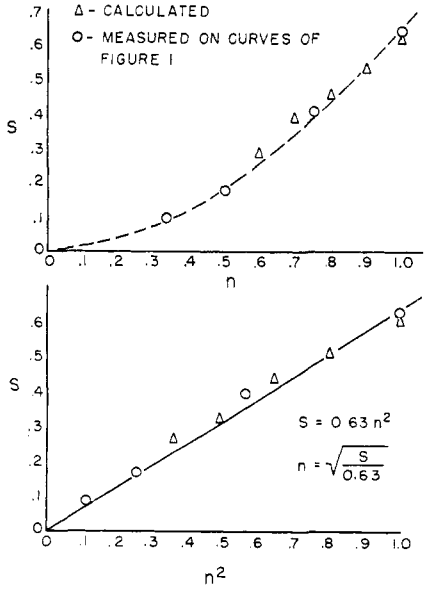

Figure 3. Values of shape index S plotted as functions of n and n^2

If the temperature rises during the reaction, the reaction rate dx/dt will rise to a maximum value, then return to zero as the reactant is exhausted. The maximum rate occurs when $d/dt\ (dx/dt)$ is zero. If the temperature rises at a constant rate ϕ, then by differentiation of Equation 7,

$$\frac{d}{dt}\left(\frac{dx}{dt}\right) = \frac{dx}{dt}\left(\frac{E\phi}{RT^2} - An(1-x)^{n-1}e^{-\frac{E}{RT}}\right) \quad (8)$$

The maximum rate occurs at a temperature T_m defined by setting Equation 8 equal to zero.

$$\frac{E\phi}{RT_m^2} = An(1-x)_m^{n-1}e^{-\frac{E}{RT_m}} \quad (9)$$

This expression is similar to that derived for the first-order case (*14*), differing only in that Equation 9 contains the product $n(1-x)_m^{n-1}$. The temperature T_m is the sample temperature at which the peak differential thermal analysis deflection occurs. The amount of material left unreacted, $(1-x)_m$, is not readily determined from the differential thermal analysis pattern.

Equation 7 can be integrated, assuming a constant heating rate, to obtain the extent of reaction as a function of temperature. The resulting integral is an exponential integral and a simple expression can not be obtained. A satisfactory approximation was obtained by Murray and White (*14*) by successive integration by parts. A rapidly converging series results, so that with little error all terms after the second may be dropped. Using Murray and White's expression, integration of Equation 7 results in

$$\frac{1}{n-1}\left(\frac{1}{(1-x)^{n-1}} - 1\right) = \frac{ART^2}{E\phi}e^{-\frac{E}{RT}}\left(1 - \frac{2RT}{E}\right) \quad (10)$$

For the special case $n = 0$, the integration yields

$$x = \frac{ART^2}{E\phi}e^{-\frac{E}{RT}}\left(1 - \frac{2RT}{E}\right) \quad (11)$$

and for the special case $n = 1$,

$$\ln\left(\frac{1}{1-x}\right) = \frac{ART^2}{E\phi}e^{-\frac{E}{RT}}\left(1 - \frac{2RT}{E}\right) \quad (12)$$

At a temperature T_m defined by Equation 9, the value of $(1-x)_m$ is given by Equation 10. If Equation 9 is combined with Equation 10, the following result is obtained, applicable for n not equal to zero or unity,

$$\frac{1}{n-1}\left(\frac{1}{(1-x)_m{}^{n-1}} - 1\right) = \frac{1}{n}\frac{1}{(1-x)_m{}^{n-1}}\left(1 - \frac{2RT_m}{E}\right) \quad (13)$$

which simplifies to

$$n(1-x)_m{}^{n-1} = 1 + (n-1)\frac{2RT_m}{E} \quad (14)$$

Equation 14 does not contain the heating rate ϕ except as T_m varies with heating rate. The product $n(1-x)_m{}^{n-1}$ is not only independent of ϕ, but is very nearly equal to unity. Substituting this value in Equation 9 and differentiating, neglecting small quantities, then

$$\frac{d\left(\ln\frac{\phi}{T_m^2}\right)}{d\left(\frac{1}{T}\right)} = -\frac{E}{R} \quad (15)$$

regardless of reaction order. If the reaction order is zero, the peak occurs when the material is exhausted—i.e., when $x = 1$—and Equation 15 can be obtained from Equation 11. This is the same expression as derived earlier for the first-order case (*10*). Equation 15 makes possible the determination of the activation energy, E, for a simple decomposition reaction regardless of reaction order by making differential thermal analysis patterns at a number of heating rates.

EFFECT OF REACTION ORDER ON PEAK SHAPE

Equation 14 predicts that the amount of undecomposed reactant at the peak temperature will decrease as the exponent n is decreased. This implies that the corresponding differential thermal analysis peak will become increasingly asymmetric as n is decreased.

It should be possible to express the degree of asymmetry in terms of n, providing that the peak shape is independent of heating rate and the values of the kinetic constants.

In Figure 1, a series of plots of reaction rate *vs.* time for a constant heating rate is shown. The reaction order n is different for each curve. These curves clearly illustrate the increasing asymmetry as n is decreased. To quantitatively describe the peak shape a "shape index" is proposed, defined as the absolute value of the ratio of the slopes of tangents to the curve at the inflection points. This shape index is illustrated in Figure 2. It can be expressed analytically as

$$S = \left| \frac{\left(\frac{d^2x}{dt^2}\right)_1}{\left(\frac{d^2x}{dt^2}\right)_2} \right| \qquad (16)$$

where subscripts 1 and 2 refer to the value of these quantities at the inflection points—i.e., where

$$\frac{d^3x}{dt^3} = 0$$

Differentiating Equation 8 and collecting terms,

$$\frac{d^3x}{dt^3} = \left[\left(2 - \frac{1}{n}\right)\left(\frac{n}{1-x}\frac{dx}{dt}\right)^2 - \frac{3n}{1-x}\frac{dx}{dt}\frac{E\phi}{RT^2} + \left(1 - \frac{2RT}{E}\right)\left(\frac{E\phi}{RT^2}\right)^2\right]\frac{dx}{dt} \qquad (17)$$

Setting Equation 17 equal to zero and solving

$$\frac{n}{(1-x)_i}\left(\frac{dx}{dt}\right)_i = \frac{E\phi}{RT_i^2}\left(\frac{3 \pm \alpha}{\beta}\right) \qquad (18)$$

where $\alpha = \sqrt{9 - 4\left(2 - \frac{1}{n}\right)\left(1 - \frac{2RT}{E}\right)}$ (18a)

$$\beta = 2\left(2 - \frac{1}{n}\right) \qquad (18b)$$

Two inflection points were obtained only for $n > 1/2$. However, the treatment to follow ignores this limitation.

Subscript i indicates the value of the quantity at the inflection point. The value of $(1 - x)_i$, found by the same procedure as was used to obtain Equation 14, is

$$(1-x)_i = 1 - \left(\frac{n-1}{n}\right)\left(\frac{3 \pm \alpha}{\beta}\right)\left(1 - \frac{2RT_i}{E}\right) \qquad (19)$$

and is essentially a function only of n, since $\left(1 - \frac{2RT_i}{E}\right)$ differs little from unity.

From Equations 16 and 8, the shape index is

$$S = \left| \frac{\left(\frac{dx}{dt}\right)_1\left[\frac{E\phi}{RT_1^2} - \frac{n}{(1-x)_1}\left(\frac{dx}{dt}\right)_1\right]}{\left(\frac{dx}{dt}\right)_2\left[\frac{E\phi}{RT_2^2} - \frac{n}{(1-x)_2}\left(\frac{dx}{dt}\right)_2\right]} \right| \qquad (20)$$

Substituting values given by Equation 18 in Equation 20

$$S = \frac{(3-\alpha)[\beta - (3-\alpha)]}{(3+\alpha)[\beta - (3+\alpha)]}\frac{(1-x)_1}{(1-x)_2}\left(\frac{T_2}{T_1}\right)^4 \qquad (21)$$

The ratio T_2/T_1 is slightly greater than unity. Solution of the transcendental Equation 18 for various values of A, E, n, and ϕ shows that T_2/T_1 varies little from an average value of about 1.08. The shape index, S, is then a function only of the reaction order, n.

Values of S calculated from Equation 21 are plotted against n and n^2 in Figure 3. Values obtained from the curves in Figure 1 are also shown. When S is plotted against n^2 the points fall roughly on a straight line defined by

$$S = 0.63\, n^2 \qquad (22)$$

from which

$$n = 1.26\, S^{1/2} \qquad (23)$$

If this expression holds for differential thermal analysis peaks as well, it provides a method for estimating the reaction order of a particular reaction from the differential thermal analysis data.

EXPERIMENTAL PROCEDURE

The differential thermal analysis apparatus used in this study is the same as described in the previous paper (*10*). All samples were run in platinum specimen holders 1/8 inch in diameter by 1/2 inch deep. The reference material was α-aluminum oxide. Heating rates from 3° per minute to 12.5° per minute were used to determine the variation of peak temperature with heating rate. The sample temperature was recorded by a platinum–platinum 10% rhodium thermocouple at the center of the sample.

The materials chosen for this study were magnesite $MgCO_3$; calcite, $CaCO_3$; and brucite, $Mg(OH)_2$. The kaolinite and halloysite previously studied (*10*) were also examined further. In each case the mineral samples were hand picked to eliminate contaminating material, and were ground in a mortar to pass a No. 140 U. S. Standard sieve. Sample holders were filled loosely with from 60 to 100 mg. of material, depending on the sample, with no packing other than gentle tapping around the outside. This method has been found to give the most reproducible results (*10*). Using the method described by Sewell (*15*), it was found that the difference between the indicated temperature and the average sample temperature, at the peak, was about 2° C. for a 10° per minute heating rate. The standard deviation of a single measurement was about 2.2° C. (*10*), so that the difference between indicated and average sample temperature was less than the limits of precision of the experiment, and no correction was applied.

Isothermal weight-loss measurements were made for each sample at a number of temperatures. The weight change

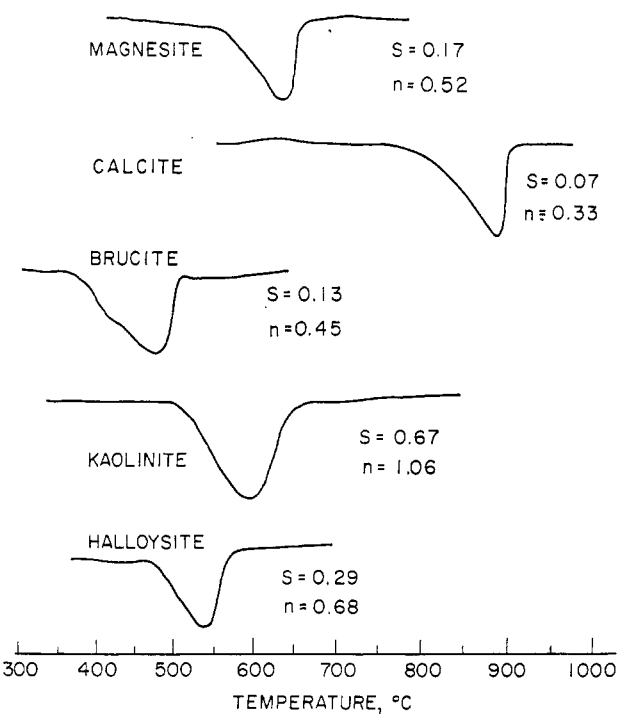

Figure 4. Typical differential thermal analysis peaks for materials used in present study

was recorded by an automatic recording balance (*12*). The isothermal weight-time records were used to determine the reaction order n by the differential method (*6*) and to obtain the reaction rate constants. The rate constants were then used to determine the activation energy and the frequency factor by graphical solution of the Arrhenius equation (*7*).

RESULTS AND DISCUSSION

The results of the differential thermal experiments with magnesite, calcite, and brucite are given in Table I. The shapes of the endothermic peaks associated with the thermal decomposition of these materials, and for kaolinite and halloysite, are given in Figure 4. Typical values of the shape index S and the corresponding n as obtained from Equation 23 are also given.

When the differential thermal data of Table I are plotted as indicated by Equation 15, straight-line plots were obtained in each case. Activation energies were then obtained from the slopes of these lines, the slopes being determined by the method of least squares. With E known, and an estimate of the value of n made, the frequency factor, A, was calculated from Equations 9 and 14.

Isothermal weight-loss measurements were used to obtain the reaction rate constants in Table II. Temperatures were measured at the center of a second sample identical in size and shape to the suspended weight-loss sample. This second sample was placed as nearly as possible in the same thermal environment as the weight-loss sample. Temperature and weight were recorded simultaneously.

The thermal decomposition of magnesite and calcite has been studied by Britton, Gregg, and Winsor (*3*). The particle size of their samples was of the order of 1 mm., and the decomposition was studied in a vacuum. The calcite decomposition has been studied by several others (*1*, *9*, *16*). Britton, Gregg, and Winsor found that for calcite the reaction order n was 0.74, and E was 41.6 kcal. per mole. Bischoff (*1*) found E to be 47 kcal. per mole in air, while Slonim (*16*) reports values from 40.8 to 44.3 kcal. per mole. For magnesite Britton, Gregg, and Winsor (*3*) report n to be 0.58 and E to be 35.6 kcal. per mole.

The thermal decomposition of brucite has been studied by Gregg and Razouk (*8*), who reported the reaction order to be 2/3 and the activation energy 27.6 kcal. per mole. Kaolinite and halloysite have been studied by Murray and White (*13*) and others. These clays are reported to decompose with n equal to unity. Activation energies vary from 35 to 45 kcal. per mole and appear to depend on the degree of crystalline order displayed by the sample.

The results of the isothermal reaction rate studies of the present work and of other workers are compared with the values obtained by the differential thermal analysis method in Table III. For magnesite, the agreement is excellent. The value of the activation energy differs slightly from that reported by Britton, Gregg, and Winsor (*3*). This discrepancy may be attributed to the difference in particle size and mineral origin in the samples.

For calcite the agreement of differential thermal analysis values with isothermal values is not as good. While the activation energies are nearly equal, there is a significant difference in the values of n measured in vacuo and in air. The probable explanation for the difference in reaction order is the ready reversibility of the reaction $CaCO_3 \rightarrow CaO + CO_2$. The carbon dioxide diffuses through the sample by a series of chemisorptions and desorptions. The decomposition which is observed in the finely divided material in air is probably influenced by the rate of diffusion of carbon dioxide gas through the sample (*5*). The reaction orders measured by the two methods in the present work are also different. It is probable that the relaxation time of the differential thermal apparatus is such that the deflection can not return to zero as abruptly as would be required by a reaction of order 0.22, the value obtained from isothermal measurements.

The activation energy of brucite obtained from differential thermal measurements differs from that obtained isothermally. The isothermal measurements confirm the findings of Gregg and Razouk (*8*), however. The differential thermal pattern of brucite exhibits a tendency toward a double peak on the endothermic deflection accompany-

Table I. Differential Thermal Analysis Results for Magnesite, Calcite, and Brucite

Heating Rate, ° C./Minute	Magnesite		Calcite		Brucite	
	T_m,[a] °C.	S[b]	T_m, °C.	S	T_m, °C.	S
3	597	0.20	871	0.06	461	0.12
4.5	615	0.22	874	0.09	469	0.11
6	626	0.17	888	0.07	484	0.13
10	642	0.21	911	0.06	494	0.16
12.5	659	0.18	927	0.07	505	0.19

[a] T_m, temperature of sample at peak.
[b] Shape index, measure of asymmetry in peak as defined in Figure 2.

Table II. Reaction Rate Constants from Weight-Loss Data

Material	Temp., ° K.	k_T, Sec.$^{-1}$
Magnesite	787	1.18×10^{-4}
	810	2.01×10^{-4}
(n = 0.55)	836	4.09×10^{-4}
	851	1.01×10^{-3}
Calcite	1079	3.22×10^{-4}
	1099	4.58×10^{-4}
(n = 0.22)	1114	5.97×10^{-4}
	1139	8.30×10^{-4}
	1152	1.03×10^{-3}
Brucite	647	4.00×10^{-4}
	670	7.34×10^{-4}
(n = 0.69)	684	1.25×10^{-3}
	720	3.15×10^{-3}

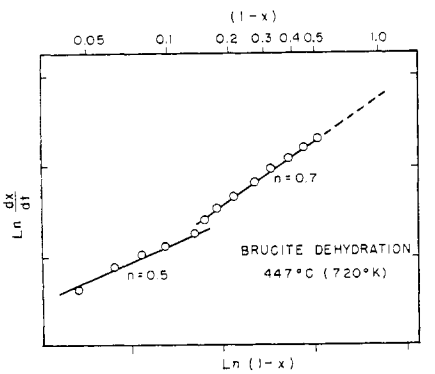

Figure 5. Reaction orders for brucite dehydration, determined from isothermal weight-loss data by differential method

Table III. Kinetic Results by Isothermal and Differential Thermal Analysis Methods

Material	Source of Data	n	ln A	E, Kcal./Mole
Magnesite	Britton, Gregg, and Winsor (*3*)	0.58	12.44	35.6
	Present work isothermal	0.55	12.63	32.5
	DTA	0.56	12.58	32.4
Calcite	Britton, Gregg, and Winsor (*3*)	0.74	10.61	41.6
	Present work isothermal	0.22	12.06	42.9
	DTA	0.32	12.31	43.7
Brucite	Gregg and Razouk (*8*)	0.67	14.73	27.6
	Present work isothermal	0.69	13.26	27.2
	DTA	0.55 to 0.44	15.18	31.4

ing the decomposition (Figure 4). Closer examination of the isothermal data reveals that there are two stages in the decomposition. Figure 5 shows one set of isothermal-weight-loss data plotted to determine reaction order by the differential method. When approximately 80% of the sample has decomposed, there is an abrupt change in reaction order from approximately 0.7 to 0.5. The change in reaction order causes a corresponding change in the differential thermal pattern, and alters the value of the reaction order obtained therefrom. The activation energy obtained by isothermal measurements is that for the reaction of order 2/3, while the differential thermal analysis method gives a value of E for the reaction of order 1/2.

Kaolinite and halloysite, both of which have been reported to decompose according to a first-order law, have been treated previously (*10*). The shape index for the kaolinite differential thermal peak is almost exactly that expected of a first-order reaction. For halloysite, however, a fractional value is indicated. Isothermal weight-loss measurements support this observation, as shown in Figure 6. The material, an Indiana halloysite, exhibits a reaction order of 1/2 when the data are plotted by the differential method. Other halloysite samples give reaction orders which are variable but are always less than unity. The difference in peak shapes has been recognized as a means for distinguishing kaolinite and halloysite for some time (*2*).

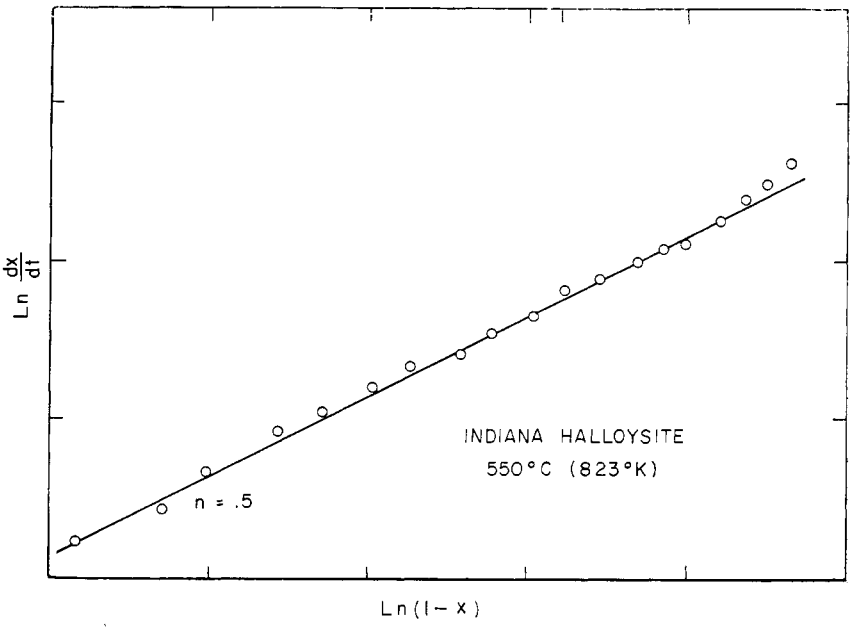

Figure 6. Reaction order for decomposition of halloysite, determined from isothermal weight-loss data by differential method

CONCLUSIONS

The method of differential thermal analysis can be used to obtain information about the kinetics and the reaction order of simple decomposition reactions. Several factors which may influence the patterns have not been examined, such as particle size, dilution, and pressure. However, the present work appears to demonstrate that the dominant factor controlling the shape and position of the differential thermal analysis peak is the nature of the reaction itself.

LITERATURE CITED

(1) Bischoff, F., *Z. anorg. Chem.* **262**, 288–96 (1950).
(2) Bramao, L., Cady, J. G., Hendricks, S. B., Swerdlow, M., *Soil Sci.* **73**, 273–87 (1952).
(3) Britton, H. T. S., Gregg, S. J., Winsor, G. W., *Trans. Faraday Soc.* **48**, 63–9 (1952).
(4) Garner, W. E., "Chemistry of the Solid State," pp. 184–211, Academic Press, New York, 1955.
(5) *Ibid.*, p. 227.
(6) Glasstone, S., "Textbook of Physical Chemistry," 2nd ed., p. 1067, Van Nostrand, New York, 1946.
(7) *Ibid.*, p. 1088.
(8) Gregg, S. J., Razouk, R. T., *J. Chem. Soc.* **1949**, S36-S44.
(9) Kappel, H., Huttig, G. F., *Kolloid-Z.* **91**, 117–34 (1940).
(10) Kissinger, H. E., *J. Research Natl. Bur. Standards* **57**, 217–21 (1956).
(11) Margenau, H., Murphy, G. M., Mathematics of Physics and Chemistry," p. 232, Van Nostrand, New York, 1943.
(12) Mauer, F. A., *Rev. Sci. Instr.* **25**, 598–602 (1954).
(13) Murray, P., White, J., *Trans. Brit. Ceram. Soc.* **54**, 151–87 (1955).
(14) *Ibid.*, p. 204–37.
(15) Sewell, E. C., *Clay Minerals Bull.* **2**, 233–41 (1955).
(16) Slonim, C., *Z. Elektrochem.* **36**, 439–53 (1930).

RECEIVED for review January 4, 1957. Accepted June 22, 1957.

Automatic Recording Buret

SAUL GORDON and CLEMENT CAMPBELL

Pyrotechnics Chemical Research Laboratory, Picatinny Arsenal, Dover, N. J.

▶ **A simply constructed automatic buret provides for the continuous graphic recording of changes in volume, with any desired electronic recorder. This apparatus can be used to measure the evolution or absorption of gases by liquid displacement, or to record the volumes of standard solution delivered during titrimetric analyses. These changes in volume can be automatically recorded as a function of physicochemical variables such as time, temperature, pH, conductivity, refractive index, electromotive force, density, or spectral transmittancy. The height of the liquid, proportional to the volume of liquid, governs the expansion of a flexible metal bellows attached to the bottom of the buret. Deflections of the bellows are measured by a linear variable differential transformer and recorded as the changes in volume.**

THE trend in modern research and development laboratories is toward the automation of the various measurements involved in obtaining both analytical and physicochemical research data. A great many of the tedious and time-consuming point-by-point manual readings have been eliminated by the use of transducers, electronic circuits, electromechanical devices, and graphic recorders, particularly in thermometry, thermogravimetry, spectrophotometry, and electrometric titrimetry. However, one of the most widely used simple laboratory tools,